

# Deportation of constant amplitude impulsive outlier (CAIO) through novel repetitive new switching-based median filtering approach

Vorapoj Patanavijit<sup>1</sup>, Kornkamol Thakulsukanant<sup>2</sup>

<sup>1</sup>Electrical and Computer Engineering, Faculty of Engineering, Assumption University of Thailand, Bangkok, Thailand

<sup>2</sup>Martin de Tours School of Management and Economics, Assumption University of Thailand, Bangkok, Thailand

## Article Info

### Article history:

Received Jun 8, 2024

Revised Sep 16, 2024

Accepted Sep 29, 2024

### Keywords:

Adaptive median filter

Digital image denoising

Digital image processing

Mean filter

NSBMF

Standard median filter

## ABSTRACT

This research paper nominates a novel repetitive new switching-based median filtering approach (R-NSBMF) for outlier deportation on computer numerical pictures that are surpassingly subverted by constant amplitude impulsive outlier (CAIO) or Salt & Pepper noise. This approach reestablishes the outlier numerical pictorial feature (which has the minimum amplitude or the maximum amplitude) by the median filter of the finite impulse response (FIR) linear predictor of all the non-outlier numerical pictorial feature in the calculating numerical pictorial division under the repetitive groundwork. The proposed R-NSBMF approach is investigated on numerous computer numerical pictures (Girl, Lena, Pepper and F16) on spacious outlier percentage and the proposed R-NSBMF approach exposes admirable outlier-deportation numerical pictures than the mean filter (mf), standard median filter (SMF), adaptive median filter (AMF), weight median filter (WMF) and original NSBMF and it professes admirable peak signal-to-noise ratio (PSNR) and pictorial quality.

*This is an open access article under the [CC BY-SA](https://creativecommons.org/licenses/by-sa/4.0/) license.*



## Corresponding Author:

Kornkamol Thakulsukanant

Martin de Tours School of Management and Economics, Assumption University of Thailand

Bangkok, Thailand

Email: kthakulsukanant@yahoo.com

## 1. INTRODUCTION

In the commonality of digital image processing and computer vision [1], there are numerous unfinished employments on computer numerical pictures [2]–[4] during the last three decades thence one of the paramount processes for unfinished computer vision employments [5] like numerous-pictures SR [6], [7], single-picture SR [8], and face verifying [9], is the outlier deportation accession because the achievement of unfinished digital image processing accessions [5]–[9] spontaneously deteriorates when these accessions implement on outlier occurrence. Under the occurrence, the outlier deportation accession is one of the paramount processes for unfinished computer vision employments thus these are numerous discoveries for progressing outlier deportation accessions, which are naturally made of an outlier uncovering accession and of an outlier deportation accession. Since 1975, the pioneer standard median filter (SMF) [10] has antecedently raised for deporting constant amplitude impulsive outlier (CAIO) and, later, has been spread to be one of the terrific admirable outlier deportation accession. For deporting CAIO on color pictures, the vector median filter (VMF) [11], which has spread from the pioneer median filter, has been raised to be one of the terrific admirable outlier deportation accession for color pictures. Subsequently, an adaptive median filter (AMF) [12], which has spread from the SMF with an enriching growth window, was raised for deporting CAIO in 1994 and, thereafter, has spread to be one of the terrific admirable outlier deportation

accession for monochrome pictures with the terrific pictorial quality. In 2017, the outlier deportation accession [13] stabilized on both a magnitude reservation cast deportation and a swarm maximization for color pictures was raised. Abruptly, automatic adjustment supporting investigation accession [14] stabilized on both a SVM regulation for MRI brain pictures was raised in 2017. Latterly, the outlier deportation accession [15] stabilized on outlier magnitude approximation in provincial window stochastic was raised for computer numerical pictures in 2018. In 2018, the outlier deportation accession [16] stabilized on an exquisite filtering accession was afterward raised for color pictures. Following, the different outlier deportation accession [17] stabilized on the composite of the Wiener filtering and Gaussian filtering was mathematically resolved the attainment by fluttering filter kernel condition in 2019. For implementing on medical MMG pictures, the outlier deportation accession [18] stabilized on the filtering accession was mathematically resolved in 2019. The numerous outlier deportation accessions stabilized on distinct techniques are mathematically overviewed on each profitable indicator by Charmouti *et al.* [19] in 2019. In 2020, another outlier deportation accession stabilized on a dismembered wavelet transform [20], which is spread from Haar wavelet transform as subdivision order by a LP filtering creation with the delay accession, was raised. For implementing on underwater outlier sounds, the outlier deportation accession stabilized on DWT [21] with numerous outliers uncovering accessions was raised in 2020. In this research paper, we review the outlier problem in the digital image processing and numerous classic and stage-of-art of outlier deportation accessions in general perspective during the last decades in the section 1. Later, section 2 expresses the numerous researches on contemporary outlier deportation accession in an impulsive outlier perspective during the last decade. As a result, the proposed outlier deportation accession based on R-NSBMF is expressed in section 3. In order to verify the performance of proposed outlier deportation accession, section 4 expresses the comparative simulation experiments obtained by using the proposed outlier deportation accessions based on R-NSBMF in contrast with the mean filter (MF), SMF, AMF, weight median filter (WMF) and original NSBMF. From these simulation experiment, the final Section expresses the conclusion and the future research.

## 2. THE CONCEPT OF CONTEMPORARY OUTLIER DEPORTATION ACCESSION

In 2017, the outlier deportation accessions stabilized on an in-cross statistical technique [22] was raised for deporting an impulsive outlier. The primary contribution of this research [22] is desired for color pictures under CAIO however this research is simulated only on one color picture (Lena) at only one outlier density. For implementing on burdensome outlier percentage of CAIO in 2017, another outlier deportation accessions, so called adaptive decision based inverse distance weighted interpolation (DBIDWI) accession [23], [24], which was raised by Kishorebabu *et al.* [23], was mathematically resolved its admirable profitable indicator [24] on spacious outlier percentages of CAIO in 2019. The primary contribution of this research [23], [24] is desired for gray pictures under CAIO at only high density-outlier however this research is not desired for spacious-density outlier, especially for low-density outlier. Abruptly, in 2019, numerous outlier deportation accessions [25] stabilized on ROAD, ROLD and RORD are mathematically resolved its admirable profitable indicator on spacious outlier percentages of CAIO. The primary contribution of this research [25] is the comparative statistical distribution of these three noise detections (ROAD, ROLD and RORD) for only outlier uncovering on gray pictures under CAIO however this research does not present overall outlier deportation accessions. Later, the outlier deportation accessions [26] stabilized on triple threshold statistical detection (TTSD) technique was raised for random amplitude impulsive outlier (RAIO) in 2018. The primary contribution of this research [26] is desired for gray pictures under RAIO at only high density-outlier (up to 80%) however this research is not desired for spacious-density outlier, especially for low-density outlier. In 2021, the outlier deportation accession [27] stabilized on sparsity weighted encoding and self-similarity priors regularization for implementing on the combination of Gaussian outlier and impulsive outlier. The primary contribution of this research [27] is desired for gray pictures under CAIO at the combination of Gaussian outlier and impulsive outlier however this research is compared with only one previous accession (A weighted encoding with sparse nonlocal regularization (WESNR), which is proposed in 2014). In 2021, the outlier deportation accessions [28] stabilized on adaptive median based non-local low rank approximation (AMNLRA) approach was raised for deporting an impulsive outlier. The primary contribution of this research [28] is desired for gray pictures under Gaussian noise and salt-and-pepper noise at low density-outlier (at 30%, 40% and 50%) however this research is not implemented on spacious-density outlier, especially high-density outlier. In 2022, the outlier deportation accessions stabilized [29] on bat algorithm (BA) and genetic algorithm (GA) for deporting an impulsive outlier. The primary contribution of this research [29] is desired for medical pictures (CT and MRI images) under Gaussian noise and salt-and-pepper noise at low density-outlier (up to 50%) however this research is not desired for spacious-density outlier, especially high-density outlier. For implementing on grayscale pictures and medical pictures with

CAIO, the outlier deportation accessions [30] stabilized on linear regression and a mean filter technique was raised for CAIO in 2022. The primary contribution of this research [30] is desired from grayscale and medical images under CAIO at large data set (TESTIMAGES) however this research has a low performance for high density-outlier. In 2023, the outlier deportation accessions [31] stabilized on AMF approach and hybrid conjugate gradient approach was raised for deporting an impulsive outlier. The primary contribution of this research [31] is desired for gray pictures under CAIO at only high density-outlier (up to 80%) however this research is not desired for spacious-density outlier, especially low-density outlier. Next, the outlier deportation accessions [32] stabilized on the Hessian cost function with the conjugate coefficient optimization in 2023. This accession was mathematically resolved its admirable profitable indicator on numerical pictures with few outlier percentages of CAIO. The primary contribution of this research [32] is desired for gray pictures under CAIO however this research is simulated only high density-outlier (at 50%, 70% and 90%). Latterly, the outlier deportation accessions stabilized on new switching-based median filtering scheme [33], which is stabilized on from the median filter of the finite impulse response (FIR) linear predictor, was first raised by Jayaraj and Ebenezer [33] for only high outlier percentages of CAIO and, later, mathematically resolved its admirable profitable indicator on four pictures with spacious outlier percentages of CAIO [34]. The primary contribution of this research [33], [34] is desired for gray pictures under CAIO however this research has a low performance for high density-outlier. As a result, some outlier deportation accession has an admirable performance on only high or only low outlier percentage but there is no outlier deportation accession with admirable performance on spacious outlier percentage. While earlier studies in the NSBMF approach have explored the impact of outlier/non-outlier neighboring elements (or outlier percentage), they have not explicitly addressed its influence on outlier/non-outlier neighboring elements.

**3. THE CONCEPT OF NOVEL REPETITIVE NEW SWITCHING-BASED MEDIAN FILTERING APPROACH**

The main contribution of this paper is to propose the novel outlier deportation accessions for CAIO or Salt & Pepper noise, which is expressed in the following subdivision. Moreover, the next contribution of this paper is to propose the simulation experiments, which are investigated on numerous computer numerical pictures, in contrast with the MF, SMF, AMF, WMF and original NSBMF, which is expressed in the next subdivision. The main concept of linear prediction (LP) is to determine the estimated data  $y(n + 1)$ , which is stabilized on linear composition (FIR linear predictor) of the previous p data from  $y(n)$  to  $y(n - p + 1)$ :

$$\hat{y}(n + 1) = \sum_{k=0}^{p-1} h(k)y(n - k) \tag{1}$$

where  $h(k)$  are the coefficients of the LP filter.

Assume that the computer numerical pictures can be formulated as the auto regressive moving average (ARMA) accession with a acknowledged system function  $p(z) = \sigma_0^2 Q(z)Q^* \left(\frac{1}{z}\right)$  such that where  $Q(z)$  is the minimum phase characteristic and  $\sigma_0^2$  is the variance of the white outlier model. For the causal infinite impulse response (IIR) filter is given by  $H(z) = z \left(\frac{1-z^{-1}}{Q(z)}\right)$ , the computer pictorial element  $\hat{y}(n + 1)$  can be mathematical determined as:

$$\hat{y}(n + 1) = \sum_{k=0}^{N-1} a_k \hat{y}(n - k) + \sum_{k=0}^{N-1} b_k y(n - k) \tag{2}$$

the mathematical determination of the proposed outlier deportation accession stabilized on from the median filter of the finite impulse can be presented as following in Figure 1:

- Sub-accession 1. An determination window ( $W_{N \times N}$ ) is picked to be  $3 \times 3$ .
- Sub-accession 2. If the picked computer pictorial element  $Y(i,j)$  is within the minimum magnitude and maximum magnitude [0 255] then this computer pictorial element is uncovered as a non-outlier element.
- Sub-accession 3. If all computer pictorial elements of 2D-configuration ( $W_{N \times N}$ ) are uncovered as outlier elements where  $Y(i,j)$  is the center location then process Sub-Accession 11. The picked computer pictorial element  $Y(i,j)$  is within the minimum magnitude and maximum magnitude [0 255] then this computer pictorial element is uncovered as a non-outlier element.
- Sub-accession 4. In different circumstances, this element  $Y(i,j)$  is uncovered as an outlier element and deported by the determined non-outlier magnitude using the ARMA.
- Sub-accession 5. Convert all computer pictorial elements of 2D-configuration  $W_{N \times N}$  to be a 1D-configuration  $Y_A$ .
- Sub-accession 6. Sort every element of a 1D-configuration  $Y_A$  from minimum magnitude to maximum magnitude.

Sub-accession 7. For each computer pictorial elements  $y(n)=255$ , the one step finite impulse response linear predictor (FRL-FIRLP) is determined from left to right and determined  $x(n)$  by (3)-(6).

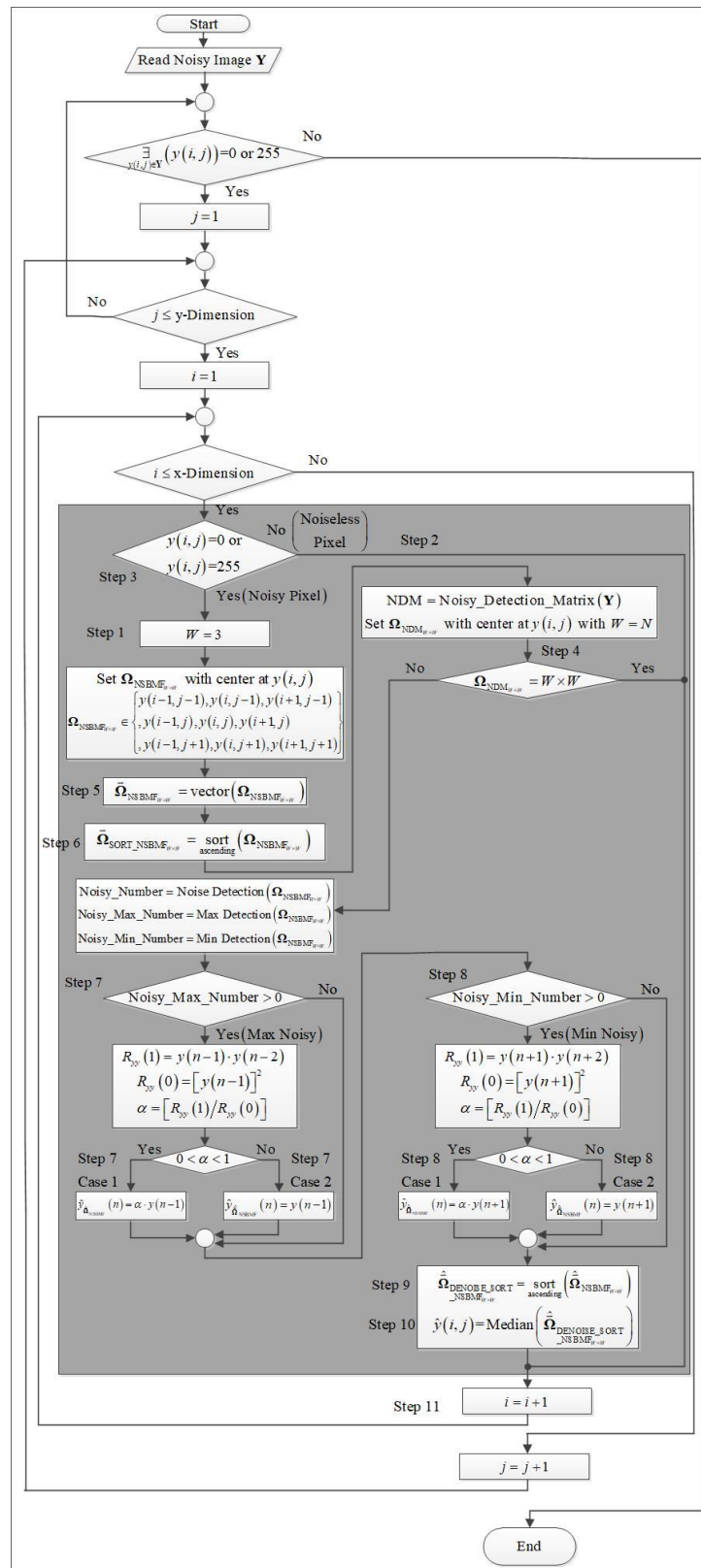


Figure 1. The corresponding flow diagram of the novel R-NSBMF approach

$$R_{yy}(1) = y(n - 1) \cdot y(n - 2) \tag{3}$$

$$R_{yy}(0) = y(n - 1) \cdot y(n - 1) \tag{4}$$

$$y(n) = \alpha \cdot y(n - 1) \text{ for } 0 < \alpha < 1, \text{ where } \alpha = \left[ \frac{R_{yy}(1)}{R_{yy}(0)} \right] \tag{5}$$

$$y(n) = y(n - 1) \text{ for } \alpha = 0 \tag{6}$$

Sub-accession 8. For each computer pictorial element  $y(n)=0$ , the FRL-FIRLP is determined from right to left and determined  $y(n)$  by:

$$R_{yy}(1) = y(n + 1) \cdot y(n + 2) \tag{7}$$

$$R_{yy}(0) = y(n + 1) \cdot y(n + 1) \tag{8}$$

$$y(n) = \alpha \cdot y(n + 1) \text{ for } 0 < \alpha < 1, \text{ where } \alpha = \left[ \frac{R_{yy}(1)}{R_{yy}(0)} \right] \tag{9}$$

$$y(n) = y(n + 1) \text{ for } \alpha > 1 \tag{10}$$

Sub-accession 9. The new vector is  $Z_A$  is determined by sorting from the determined vector  $Y_A$ , which is determined by the FRL-FIRLP model.

Sub-accession 10. The deportation computer pictorial element  $\hat{y}(n)$  is determined by the median of the sorted vector is  $Z_A$ .

Sub-accession 11. Sub-Accession 1 to Sub-Accession 3 are repeated for all computer pictorial elements.

#### 4. THE SIMULATION EXPERIMENT

In this subdivision of simulation experiments, the computational application is the MATLAB, which is stabilized and accomplished on numerical office-computers at mechanical particularizations: primary operating chip i7-6700HQ with primary storage 16 GB RAM. Distinct office-computers are simulationally operated on numerical pictures, which are constructed of Girl, Lena, Pepper and F16, and all numerical pictures are fabricated by adding the CAIO at spacious outlier percentages (5%-90%). For outlier distinct ubiquitous spacious of outlier percentages, experiment repercussion of functioning in PSNR of the R-NSBMF approach on numerical pictures: Girl, Lena, Pepper and F16 are simulationally operated in Tables 1-4, subsequently. For revealing the outlier functioning, the proposed outlier deportation accession stabilized on R-NSBMF approach are simulationally operated in contradicting with numerical other outlier deportation accessions: 3×3-SMF [10], 3×3-MF [1], AMF [12], 3×3- weight median filter (WMF) [1], 5×5-WMF [1] and NSBMF approach [33], [34].

As experiment repercussions on Girl picture in Table 1, the functioning of the outlier deportation accessions of R-NSBMF has an admirable signal-to-noise-ratio (in Decibel) in above contradicting with 3×3-MF, 3×3-SMF, AMF, 3×3-WMF, 5×5-WMF and NSBMF functioning of roughly 21.6015±0.7134 dB, 16.2454±4.9815 dB, 8.4869±3.6881 dB, 15.0306±5.9837 dB, 9.9382±6.1273 dB, 9.1071±6.8111 dB, subsequently. As experiment repercussions on Lena picture in Table 2, the functioning of the outlier deportation accessions of R-NSBMF has an admirable signal-to-noise-ratio (in Decibel) in above contradicting with 3×3-MF, 3×3-SMF, AMF, 3×3-WMF, 5×5-WMF and NSBMF functioning of roughly 18.0808±1.4814 dB, 13.7265±3.8566 dB, 7.8938±2.6605 dB, 13.0872±4.1864 dB, 9.0731±4.4540 dB, 4.4547±5.3889 dB, subsequently. As experiment repercussions on Pepper picture in Table 3, the functioning of the outlier deportation accessions of R-NSBMF has an admirable signal-to-noise-ratio (in Decibel) in above contradicting with 3×3-MF, 3×3-SMF, AMF, 3×3-WMF, 5×5-WMF and NSBMF functioning of roughly 17.9388±1.6415 dB, 13.6807±3.5884 dB, 7.5873±2.6716 dB, 12.8006±4.1037 dB, 8.9452±4.2582 dB, 4.2953±5.1814 dB, subsequently. As experiment repercussions on F16 picture in Table 4, the functioning of the outlier deportation accessions of R-NSBMF has an admirable signal-to-noise-ratio (in Decibel) in above contradicting with 3×3-MF, 3×3-SMF, AMF, 3×3-WMF, 5×5-WMF and NSBMF functioning of roughly 18.6021±1.2259 dB, 14.0848±3.9633 dB, 7.8410±2.9779 dB, 9.8274±3.2653 dB, 7.8767±2.9856 dB, 4.5751±5.4741 dB, subsequently. For outlier distinct ubiquitous spacious of outlier percentages, experiment repercussion of functioning in SSIM of the R-NSBMF approach on numerical pictures: Girl, Lena, Pepper and F16 are simulationally operated in Tables 5-8, subsequently. For revealing the outlier functioning, the

proposed outlier deportation accession stabilized on R-NSBMF approach are simulationally operated in contradicting with numerical other outlier deportation accessions: 3×3-SMF, 3×3-MF, AMF, 3×3-WMF, 5×5-WMF and NSBMF approach. As experiment repercussions on Girl picture in Table 5, the functioning of the outlier deportation accessions of R-NSBMF has an admirable SSIM in above contradicting with 3×3-MF, 3×3-SMF, AMF, 3×3-WMF, 5×5-WMF and NSBMF functioning of roughly 0.6664±0.1521 dB, 0.7849±0.0669 dB, 0.2327±0.1896 dB, 0.4872±0.3160 dB, 0.2796±0.2782 dB, 0.2772±0.2915 dB, subsequently.

Table 1. The experiment repercussion of functioning of the R-NSBMF in PSNR (Girl)

Experimental picture	Outlier percentage (%)	Outliered picture	PSNR (dB)						
			3×3 MF (mean filter)	3×3 SMF (median filter)	AMF	3×3 WMF	5×5 WMF	NSBMF	R-NSBMF
Girl (256×256)	D=5	16.4490	20.0454	32.4867	37.5518	35.9690	36.3119	40.5367	40.4905
	D=10	13.6890	17.2530	31.5583	36.8900	34.0977	34.1081	38.9342	38.9017
	D=15	11.9287	15.3515	27.6179	34.8060	31.1067	32.7037	37.2431	37.1356
	D=20	10.6567	13.9593	25.5153	32.0377	28.0604	31.3171	33.9590	35.9738
	D=25	9.5498	12.7248	22.9614	29.6044	24.8722	30.8000	32.2765	34.9497
	D=30	8.8677	11.9599	20.7738	27.6911	22.2937	29.7153	30.7784	34.2409
	D=35	8.0984	11.0501	18.4410	24.9701	19.3002	28.6972	28.0345	33.0135
	D=40	7.5798	10.4543	16.5146	23.3733	17.0943	27.6109	25.7346	32.6008
	D=45	7.0728	9.8471	14.8145	21.8116	15.2681	25.5460	23.8902	32.2653
	D=50	6.5712	9.2367	13.0319	20.1711	13.3881	23.4389	20.9953	31.2744
	D=55	6.2085	8.7895	11.8226	19.2184	12.1602	20.8704	19.6609	30.7265
	D=60	5.8609	8.3590	10.4981	18.4518	10.9121	17.8824	17.2885	30.2195
	D=65	5.4832	7.8712	9.1396	17.2740	9.6478	15.1961	15.4827	29.6338
	D=70	5.1311	7.4271	8.0463	16.7334	8.5653	12.7541	13.5364	29.0393
	D=75	4.8712	7.0814	7.1994	16.2921	7.7377	10.9117	12.0920	28.3270
	D=80	4.5674	6.6881	6.2520	16.2795	6.8373	9.0411	10.1641	27.8348
D=85	4.3054	6.3340	5.4218	16.5924	6.0352	7.4206	8.2711	26.8128	
D=90	4.0573	5.9986	4.7465	16.7463	5.3617	6.0460	6.8258	25.8186	

Table 2. The experiment repercussion of functioning of the R-NSBMF in PSNR (Lena)

Experimental picture	Outlier percentage (%)	Outliered picture	PSNR (dB)						
			3×3 MF (mean filter)	3×3 SMF (median filter)	AMF	3×3 WMF	5×5 WMF	NSBMF	R-NSBMF
Lena (256×256)	D=5	18.7139	22.4181	31.6421	36.0907	35.1721	34.5535	43.3767	43.3767
	D=10	15.6564	19.3812	30.7076	35.3032	32.4698	32.2808	39.4824	39.4824
	D=15	13.8274	17.5385	29.2982	33.7454	30.2208	31.1339	37.1963	37.1963
	D=20	12.6389	16.3208	27.6257	32.1558	28.3548	30.3752	35.5897	35.5897
	D=25	11.6783	15.3526	25.4101	29.8105	25.8645	29.5861	34.1799	34.2972
	D=30	10.8971	14.5829	23.6811	27.9141	23.9839	28.8233	33.3666	33.5017
	D=35	10.2240	13.8785	20.8127	25.6654	21.1014	28.1014	32.1569	32.2703
	D=40	9.6481	13.2479	19.0080	23.7903	19.1825	27.2510	30.9519	31.6218
	D=45	9.0745	12.6598	16.8389	21.5949	16.9429	25.6878	29.8758	30.8787
	D=50	8.6553	12.2146	15.4758	20.5725	15.5050	23.7318	28.3305	30.3551
	D=55	8.2118	11.7609	13.8573	19.4896	13.9115	21.4153	26.5398	29.7866
	D=60	7.7813	11.2939	12.3280	18.1747	12.5485	18.6948	23.8235	28.9900
	D=65	7.4884	11.0012	11.3251	17.7283	11.5932	16.7976	21.1663	28.4283
	D=70	7.1697	10.6509	10.2861	17.1153	10.6427	14.7470	19.0147	27.7841
	D=75	6.8497	10.2599	9.1271	16.5388	9.5848	12.3932	16.3975	27.0012
	D=80	6.5846	10.0057	8.3331	16.4554	8.8622	10.8970	14.0686	26.3088
D=85	6.3241	9.7338	7.5344	16.4230	8.1548	9.3376	11.8418	25.7675	
D=90	6.0604	9.4356	6.8241	16.5352	7.5261	8.0678	9.6484	24.5552	

Table 3. The experiment repercussion of functioning of the R-NSBMF in PSNR (Pepper)

Experimental picture	Outlier percentage (%)	Outliered picture	PSNR (dB)						
			3×3 MF (mean filter)	3×3 SMF (median filter)	AMF	3×3 WMF	5×5 WMF	NSBMF	R-NSBMF
Pepper (256×256)	D=5	18.4752	22.1408	32.2578	37.1145	35.0049	33.6748	43.3656	43.3656
	D=10	15.3798	19.0677	30.6116	36.0391	32.6811	31.8203	39.3957	39.3957
	D=15	13.5570	17.2234	28.8470	33.6095	30.4266	30.7565	36.9922	36.9922
	D=20	12.3593	15.9804	26.5888	31.6485	28.3098	29.8638	34.8186	34.8186
	D=25	11.3929	14.9986	24.2073	29.4205	25.2232	28.9233	33.6034	33.6747
	D=30	10.6242	14.1748	22.0663	26.7650	23.0148	28.4090	32.8543	32.9228
	D=35	9.9742	13.5209	20.3774	25.5249	21.0650	27.8691	31.5910	31.9301
	D=40	9.3998	12.9076	18.4321	23.4995	18.8546	26.9506	30.8539	31.1997
	D=45	8.8599	12.3275	16.6168	21.7177	16.9821	25.0508	29.4292	30.2782
	D=50	8.3843	11.8117	14.8506	20.2203	15.0906	23.3417	27.8805	29.9773
	D=55	7.9930	11.3720	13.4655	19.0894	13.7177	21.2505	25.9102	29.2980
	D=60	7.6189	10.9563	12.0128	18.1116	12.3715	18.5046	23.3946	28.4030
	D=65	7.2684	10.5758	10.8920	17.3657	11.2881	16.2700	21.0225	27.9090
	D=70	6.9246	10.2039	9.7704	16.5923	10.2656	14.0814	18.5155	27.1854
	D=75	6.6418	9.8955	8.8751	16.2338	9.4361	12.5170	16.2277	26.5085
	D=80	6.3710	9.5853	8.0166	16.0896	8.6043	10.6953	13.8081	25.6540
	D=85	6.1097	9.2949	7.2402	16.0498	7.8970	9.0864	11.5906	24.7030
D=90	5.8582	9.0214	6.5767	16.2932	7.3127	7.8774	9.3874	23.7409	

Table 4. The experiment repercussion of functioning of the R-NSBMF in PSNR (F16)

Experimental picture	Outlier percentage (%)	Outliered picture	PSNR (dB)						
			3×3 MF (mean filter)	3×3 SMF (median filter)	AMF	3×3 WMF	5×5 WMF	NSBMF	R-NSBMF
F16 (256×256)	D=5	17.9498	21.5802	31.4106	36.6062	35.0562	33.9410	43.4116	43.4116
	D=10	14.8320	18.4426	29.6532	34.6310	32.8038	32.0086	37.7960	37.7960
	D=15	13.1197	16.6870	28.3176	33.5561	31.4609	30.6870	36.2753	36.2753
	D=20	11.8045	15.3181	26.4356	31.3844	29.6277	29.7829	34.6905	34.6905
	D=25	10.9272	14.3866	24.4147	29.5029	27.6540	29.0736	33.5909	33.5909
	D=30	10.0510	13.4526	21.8862	27.1347	25.5386	27.8733	32.2724	32.4947
	D=35	9.4325	12.7646	19.6835	25.0118	23.7815	27.0371	31.4697	31.8633
	D=40	8.8735	12.1397	17.6412	23.0147	22.1737	25.9942	30.0454	30.7706
	D=45	8.3344	11.5224	15.8686	21.2768	20.2179	24.7055	29.3263	30.4606
	D=50	7.8600	11.0091	14.2697	19.6201	19.0001	23.3418	27.5389	29.7043
	D=55	7.4696	10.5769	12.8823	18.6408	17.4576	21.3622	25.4928	29.0693
	D=60	7.0920	10.1202	11.5290	17.6586	16.2979	19.7167	23.2711	28.2709
	D=65	6.7276	9.7008	10.4080	16.9400	15.1766	18.0660	20.7034	27.9558
	D=70	6.4128	9.3238	9.3042	16.2514	14.2170	16.5416	18.2121	27.4542
	D=75	6.1274	9.0020	8.3797	15.9223	13.3259	15.1864	15.8585	26.7143
	D=80	5.8647	8.6893	7.5835	15.7428	12.3822	13.8615	13.5849	26.0167
	D=85	5.5768	8.3346	6.7043	15.8098	11.7633	12.9123	11.0516	25.2379
D=90	5.3335	8.0381	6.0278	16.0834	11.0983	12.0537	8.9823	24.1494	

As experiment repercussions on Lena picture in Table 6, the functioning of the outlier deportation accessions of R-NSBMF has an admirable SSIM in above contradicting with 3×3-MF, 3×3-SMF, AMF, 3×3-WMF, 5×5-WMF and NSBMF functioning of roughly 0.3847±0.2871 dB, 0.7031±0.0922 dB, 0.2477±0.1878 dB, 0.4863±0.2851 dB, 0.3095±0.2610 dB, 0.1835±0.2500 dB, subsequently. As experiment repercussions on Pepper picture in Table 7, the functioning of the outlier deportation accessions of R-NSBMF has an admirable SSIM in above contradicting with 3×3-MF, 3×3-SMF, AMF, 3×3-WMF, 5×5-WMF and NSBMF functioning of roughly 0.3870±0.2901 dB, 0.7084±0.0961 dB, 0.2355±0.1878 dB, 0.4817±0.2936 dB, 0.3060±0.2643 dB, 0.1837±0.2513 dB, subsequently. As experiment repercussions on F16 picture in Table 8, the functioning of the outlier deportation accessions of R-NSBMF has an admirable

SSIM in above contradicting with 3×3-MF, 3×3-SMF, AMF, 3×3-WMF, 5×5-WMF and NSBMF functioning of roughly 0.4265±0.3048 dB, 0.7468±0.0829 dB, 0.2812±0.2193 dB, 0.4989±0.3112 dB, 0.3146±0.2822 dB, 0.1976±0.2711 dB, subsequently.

Table 5. The experiment repercussion of functioning of the R-NSBMF in SSIM (Girl)

Experimental picture	Outlier percentage (%)	Outliered picture	SSIM						
			3×3 MF (mean filter)	3×3 SMF (median filter)	AMF	3×3 WMF	5×5 WMF	NSBMF	R-NSBMF
Girl (256×256)	D=5	0.3479	0.4186	0.6675	0.9898	0.9592	0.9665	0.9825	0.9827
	D=10	0.2187	0.2766	0.5522	0.9886	0.9414	0.9445	0.9763	0.9764
	D=15	0.1642	0.2120	0.4897	0.9831	0.9054	0.9306	0.9697	0.9698
	D=20	0.1282	0.1685	0.4456	0.9705	0.8683	0.9122	0.9535	0.9615
	D=25	0.1062	0.1417	0.3972	0.9454	0.8054	0.8970	0.9388	0.9524
	D=30	0.0914	0.1227	0.3478	0.9014	0.7330	0.8808	0.9239	0.9448
	D=35	0.0789	0.1070	0.3019	0.8536	0.6146	0.8618	0.8952	0.9340
	D=40	0.0659	0.0903	0.2465	0.7769	0.4883	0.8361	0.8441	0.9253
	D=45	0.0581	0.0800	0.1854	0.6884	0.3647	0.7986	0.7940	0.9146
	D=50	0.0526	0.0730	0.1441	0.6205	0.2524	0.7442	0.6989	0.9032
	D=55	0.0464	0.0651	0.1075	0.5512	0.1720	0.6940	0.6331	0.8931
	D=60	0.0396	0.0562	0.0799	0.4878	0.1120	0.5750	0.5130	0.8817
	D=65	0.0362	0.0515	0.0605	0.4336	0.0702	0.4340	0.3960	0.8676
	D=70	0.0314	0.0452	0.0447	0.3945	0.0443	0.2909	0.2840	0.8527
	D=75	0.0279	0.0404	0.0366	0.3714	0.0297	0.1963	0.1990	0.8379
	D=80	0.0234	0.0342	0.0262	0.3671	0.0173	0.0981	0.1042	0.8190
D=85	0.0208	0.0305	0.0219	0.3598	0.0119	0.0520	0.0467	0.7913	
D=90	0.0182	0.0270	0.0178	0.3789	0.0094	0.0240	0.0259	0.7605	

Table 6. The experiment repercussion of functioning of the R-NSBMF in SSIM (Lena)

Experimental picture	Outlier percentage (%)	Outliered picture	SSIM						
			3×3 MF (mean filter)	3×3 SMF (median filter)	AMF	3×3 WMF	5×5 WMF	NSBMF	R-NSBMF
Lena (256×256)	D=5	0.5060	0.5804	0.9783	0.9785	0.9550	0.9566	0.9938	0.9938
	D=10	0.3594	0.4295	0.9749	0.9762	0.9220	0.9281	0.9858	0.9858
	D=15	0.2768	0.3402	0.9663	0.9698	0.8734	0.9076	0.9763	0.9763
	D=20	0.2249	0.2818	0.9509	0.9546	0.8354	0.8848	0.9670	0.9670
	D=25	0.1900	0.2409	0.9039	0.9260	0.7801	0.8659	0.9570	0.9570
	D=30	0.1652	0.2124	0.8307	0.8752	0.7019	0.8497	0.9460	0.9469
	D=35	0.1431	0.1855	0.7333	0.8161	0.5662	0.8228	0.9307	0.9321
	D=40	0.1219	0.1598	0.6140	0.7319	0.4555	0.7945	0.9145	0.9217
	D=45	0.1063	0.1409	0.4893	0.6518	0.3266	0.7517	0.8935	0.9083
	D=50	0.0941	0.1254	0.3853	0.5728	0.2357	0.6948	0.8632	0.8971
	D=55	0.0787	0.1062	0.2987	0.5015	0.1600	0.5964	0.8057	0.8821
	D=60	0.0707	0.0960	0.2348	0.4454	0.1027	0.4735	0.7078	0.8610
	D=65	0.0590	0.0808	0.1823	0.3953	0.0771	0.3366	0.5845	0.8451
	D=70	0.0490	0.0682	0.1374	0.3558	0.0539	0.2246	0.4452	0.8222
	D=75	0.0466	0.0644	0.1102	0.3323	0.0385	0.1162	0.2992	0.7980
	D=80	0.0342	0.0484	0.0769	0.3163	0.0247	0.0624	0.1769	0.7702
D=85	0.0323	0.0455	0.0614	0.3127	0.0220	0.0400	0.0989	0.7391	
D=90	0.0246	0.0354	0.0431	0.3256	0.0120	0.0205	0.0473	0.6932	

The proposed approach (R-NSBMF) may benefit from the non-outlier neighboring elements without adversely impacting the impact of the outlier neighboring elements because if all neighboring elements are outlier then the computed pictorial element is not denoised until some neighboring elements are non-outlier. Furthermore, the fragmentary of the experiment repercussions of the Pepper picture, in contradicting with numerical other outlier deportation accessions: 3×3-SMF, 3×3-MF, AMF, 3×3-WMF, 5×5-WMF, and

NSBMF approach, is exposed in Figures 2-5 for 30%, 50%, 70%, and 90% outlier percentages, subsequently. (The below picture on each experiment result of each sub-picture is the absolute subtraction between it's correspond upper picture to the original picture. The subtraction is multiplied by 5).

Table 7. The experiment repercussion of functioning of the R-NSBMF in SSIM (Pepper)

Experimental picture	Outlier percentage (%)	Outliered picture	SSIM						
			3×3 MF (mean filter)	3×3 SMF (median filter)	AMF	3×3 WMF	5×5 WMF	NSBMF	R-NSBMF
Pepper (256×256)	D=5	0.5067	0.5831	0.9801	0.9948	0.9582	0.9554	0.9946	0.9946
	D=10	0.3636	0.4367	0.9737	0.9936	0.9334	0.9302	0.9879	0.9879
	D=15	0.2841	0.3501	0.9663	0.9886	0.8956	0.9114	0.9797	0.9797
	D=20	0.2328	0.2915	0.9513	0.9760	0.8576	0.8937	0.9704	0.9704
	D=25	0.1989	0.2523	0.9088	0.9504	0.7951	0.8741	0.9605	0.9611
	D=30	0.1681	0.2154	0.8359	0.9005	0.7101	0.8589	0.9536	0.9541
	D=35	0.1451	0.1880	0.7501	0.8418	0.6122	0.8431	0.9375	0.9402
	D=40	0.1289	0.1686	0.6307	0.7563	0.4791	0.8145	0.9279	0.9320
	D=45	0.1120	0.1474	0.5068	0.6805	0.3650	0.7705	0.9044	0.9178
	D=50	0.0940	0.1257	0.3966	0.6029	0.2472	0.7158	0.8731	0.9079
	D=55	0.0856	0.1146	0.3166	0.5342	0.1795	0.6301	0.8194	0.8949
	D=60	0.0727	0.0986	0.2444	0.4746	0.1216	0.4862	0.7224	0.8767
	D=65	0.0624	0.0851	0.1920	0.4206	0.0879	0.3669	0.6079	0.8606
	D=70	0.0561	0.0768	0.1502	0.3842	0.0573	0.2332	0.4685	0.8410
	D=75	0.0448	0.0620	0.1144	0.3528	0.0438	0.1471	0.3132	0.8181
	D=80	0.0399	0.0557	0.0897	0.3465	0.0307	0.0772	0.1951	0.7901
D=85	0.0330	0.0467	0.0661	0.3411	0.0231	0.0415	0.1077	0.7520	
D=90	0.0245	0.0355	0.0445	0.3472	0.0161	0.0277	0.0549	0.7057	

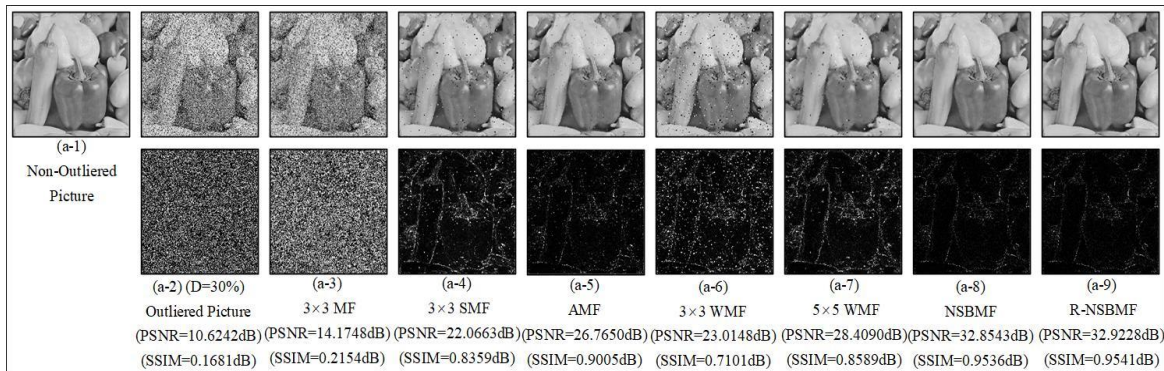


Figure 2. The experiment repercussions on Pepper picture for CAIO at 30% outlier percentages

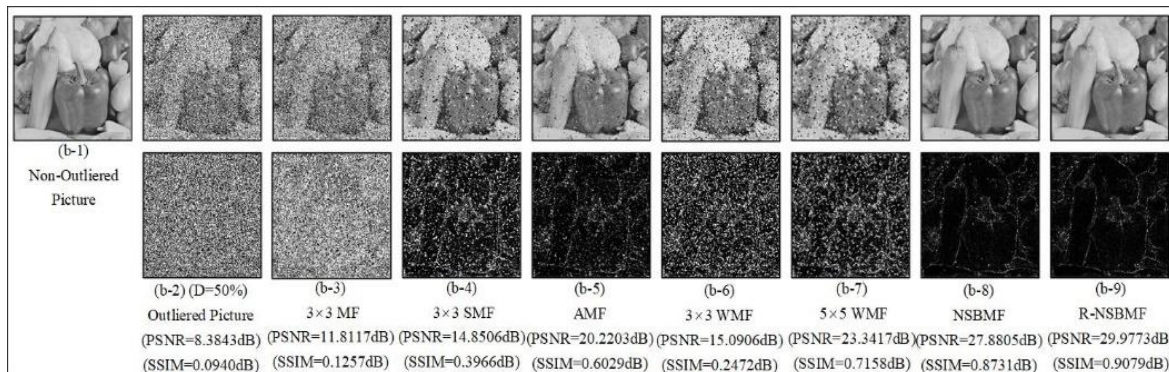


Figure 3. The experiment repercussions on Pepper picture for CAIO at 50% outlier percentages

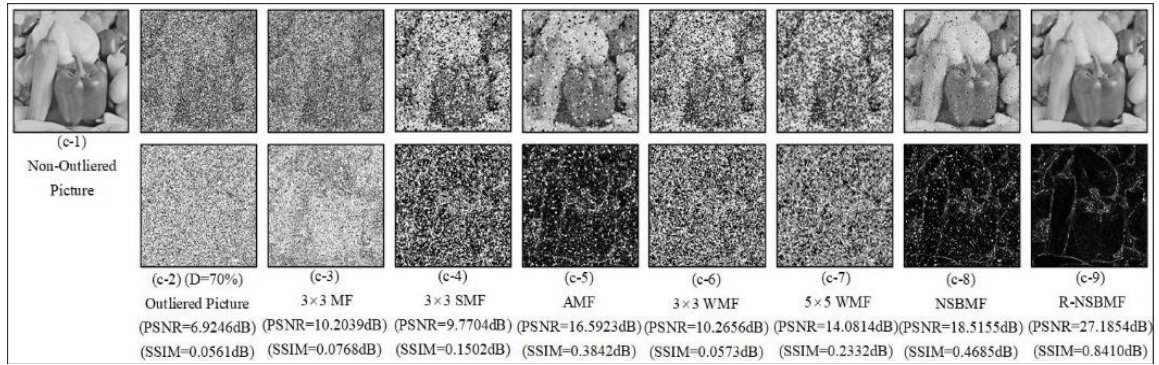


Figure 4. The experiment repercussions on Pepper picture for CAIO at 70% outlier percentages

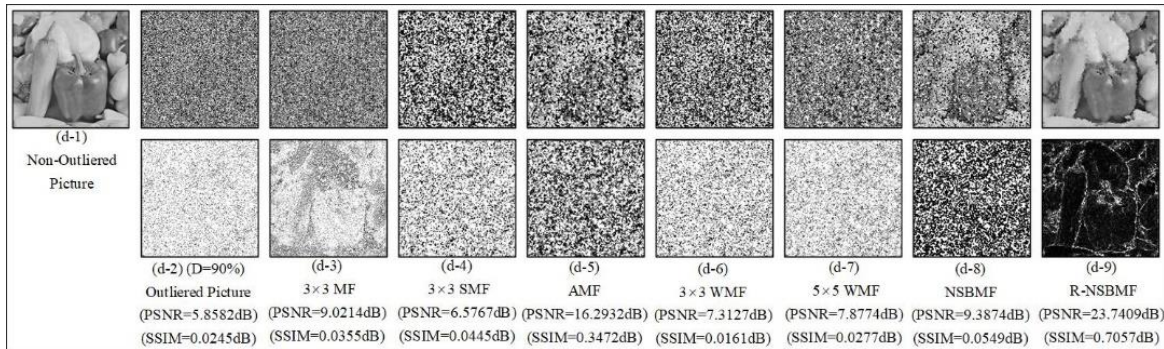


Figure 5. The experiment repercussions on Pepper picture for CAIO at 90% outlier percentages

Table 8. The experiment repercussion of functioning of the R-NSBMF in SSIM (F16)

Experimental picture	Outlier percentage (%)	Outliered picture	SSIM						
			3x3 MF (mean filter)	3x3 SMF (median filter)	AMF	3x3 WMF	5x5 WMF	NSBMF	R-NSBMF
F16 (256x256)	D=5	0.4419	0.5134	0.9762	0.9924	0.9625	0.9629	0.9951	0.9951
	D=10	0.3074	0.3702	0.9703	0.9901	0.9405	0.9387	0.9881	0.9881
	D=15	0.2395	0.2954	0.9551	0.9851	0.9049	0.9216	0.9815	0.9815
	D=20	0.1989	0.2491	0.9402	0.9731	0.8625	0.9015	0.9737	0.9737
	D=25	0.1676	0.2127	0.8918	0.9355	0.8151	0.8862	0.9665	0.9665
	D=30	0.1464	0.1877	0.8127	0.8921	0.7219	0.8690	0.9551	0.9570
	D=35	0.1239	0.1613	0.6965	0.7981	0.6005	0.8467	0.9432	0.9472
	D=40	0.1115	0.1458	0.5746	0.7273	0.4762	0.8174	0.9303	0.9377
	D=45	0.0964	0.1273	0.4596	0.6360	0.3380	0.7775	0.9105	0.9297
	D=50	0.0861	0.1142	0.3526	0.5476	0.2341	0.7223	0.8794	0.9157
	D=55	0.0757	0.1013	0.2726	0.4789	0.1630	0.6392	0.8226	0.9060
	D=60	0.0629	0.0859	0.2044	0.4246	0.1105	0.5266	0.7431	0.8925
	D=65	0.0541	0.0738	0.1563	0.3663	0.0756	0.3641	0.6123	0.8792
	D=70	0.0471	0.0650	0.1240	0.3300	0.0528	0.2284	0.4585	0.8613
	D=75	0.0433	0.0599	0.0980	0.3139	0.0369	0.1321	0.2995	0.8401
	D=80	0.0362	0.0508	0.0745	0.2961	0.0272	0.0755	0.1807	0.8207
	D=85	0.0296	0.0421	0.0567	0.2895	0.0171	0.0393	0.0923	0.7919
D=90	0.0232	0.0337	0.0387	0.3051	0.0132	0.0214	0.0443	0.7487	

### 5. CONCLUSION

This research paper engages to nominate a novel R-NSBMF, which is spread from the pioneer NSBMF approach, for outlier deportation on computer numerical pictures that are surpassingly subverted by CAIO or Salt and Pepper noise at spacious outlier percentages (5%-90%). In order to mathematically

considering the functioning of the outlier deportation accession stabilized on R-NSBMF approach are simulationally operated on Girl, Lena, Pepper and F16. From consummate experiment repercussions, the functioning of outlier deported pictures from the R-NSBMF accession has admirable signal-to-noise-ratio (in Decibel) and SSIM in contradicting with numerical other outlier deportation accessions: 3×3-SMF, 3×3-MF, AMF, 3×3-WMF, 5×5-WMF and NSBMF approach. As a result, the novel outlier deportation accessions with an admirable performance on spacious outlier percentage is proposed therefore advance digital image processing accessions, which spontaneously deteriorates when these accessions implement on outlier occurrence, can be implemented on wide-range implementations (spacious outlier percentage) with superior performance. As a result, the limitation of the novel outlier deportation accessions is the limited performance on only low outlier percentage (5%-25%), which is equally compared to the NSBMF approach. Compared with SMF of AMF, the proposed approach (R-NSBMF) has higher complexity and requires more computational time. Future studies may explore the computation of the R-NSBMF approach with feasible ways of producing the low computation and the fast calculation.

## REFERENCES

- [1] R. C. Gonzalez and R. E. Woods, *Digital image processing*, 2nd edition, New Jersey: Prentice-Hall, Upper Saddle River, 2002.
- [2] A. S. M. Shafi and M. M. Rahman, "Decomposition of color wavelet with higher order statistical texture and convolutional neural network features set based classification of colorectal polyps from video endoscopy," *International Journal of Electrical and Computer Engineering*, vol. 10, no. 3, pp. 2986–2996, Jun. 2020, doi: 10.11591/ijece.v10i3.pp2986-2996.
- [3] S. Bagchi, K. G. Tay, A. Huong, and S. K. Debnath, "Image processing and machine learning techniques used in computer-aided detection system for mammogram screening-A review," *International Journal of Electrical and Computer Engineering*, vol. 10, no. 3, pp. 2336–2348, Jun. 2020, doi: 10.11591/ijece.v10i3.pp2336-2348.
- [4] N. D. Abdullah, U. R. Hashim, S. Ahmad, and L. Salahuddin, "Analysis of texture features for wood defect classification," *Bulletin of Electrical Engineering and Informatics*, vol. 9, no. 1, pp. 121–128, Feb. 2020, doi: 10.11591/eei.v9i1.1553.
- [5] A. J. Qasim, R. Din, and F. Q. A. Alyousuf, "Review on techniques and file formats of image compression," *Bulletin of Electrical Engineering and Informatics*, vol. 9, no. 2, pp. 602–610, Apr. 2020, doi: 10.11591/eei.v9i2.2085.
- [6] V. H. Patil, and G. K. Kharate, "Super resolution imaging needs better registration for better quality results," *Bulletin of Electrical Engineering and Informatics*, vol. 1, no. 1, pp. 43–50, 2012.
- [7] C. Deng, J. Liu, W. Tian, S. Wang, H. Zhu, and S. Zhang, "Image super-resolution reconstruction based on L1/2 sparsity," *Bulletin of Electrical Engineering and Informatics*, vol. 3, no. 3, 2014, doi: 10.12928/eei.v3i3.284.
- [8] D. Kesrarat, K. Thakulsukanant, and V. Patanavijit, "A novel elementary spatial expanding scheme form on SISR method with modifying Geman&McClure function," *Telkomnika (Telecommunication Computing Electronics and Control)*, vol. 17, no. 5, pp. 2554–2560, Oct. 2019, doi: 10.12928/TELKOMNIKA.v17i5.12799.
- [9] R. S. Perumal, R. K. Nadesh, and N. C. S. Kumar, "Robust face recognition using enhanced local binary pattern," *Bulletin of Electrical Engineering and Informatics*, vol. 7, no. 1, pp. 96–101, Mar. 2018, doi: 10.11591/eei.v7i1.761.
- [10] W. K. Pratt, "Median filtering," *Image Processing Institute, University of Southern California, Los Angeles, Tech. Rep., 1975*.
- [11] J. Astola, P. Haavisto, and Y. Neuvo, "Vector median filters," *Proceedings of the IEEE*, vol. 78, no. 4, pp. 678–689, Apr. 1990, doi: 10.1109/5.54807.
- [12] H. Hwang and R. A. Haddad, "Adaptive median filters: new algorithms and results," *IEEE Transactions on Image Processing*, vol. 4, no. 4, pp. 499–502, Apr. 1995, doi: 10.1109/83.370679.
- [13] O. P. Verma and N. Sharma, "Intensity preserving cast removal in color images using particle swarm optimization," *International Journal of Electrical and Computer Engineering*, vol. 7, no. 5, pp. 2581–2595, Oct. 2017, doi: 10.11591/ijece.v7i5.pp2581-2595.
- [14] M. Hamiane and F. Saeed, "SVM classification of MRI brain images for computer-assisted diagnosis," *International Journal of Electrical and Computer Engineering (IJECE)*, vol. 7, no. 5, p. 2555, 2017, doi: 10.11591/ijece.v7i5.pp2555-2564.
- [15] A. Khmag, S. Ghoul, S. A. R. Al-Haddad, and N. Kamarudin, "Noise level estimation for digital images using local statistics and its applications to noise removal," *Telkomnika (Telecommunication Computing Electronics and Control)*, vol. 16, no. 2, pp. 915–924, Apr. 2018, doi: 10.12928/TELKOMNIKA.v16i2.9060.
- [16] K. A. Sai and K. Ravi, "An efficient filtering technique for denoising colour images," *International Journal of Electrical and Computer Engineering*, vol. 8, no. 5, pp. 3604–3608, Oct. 2018, doi: 10.11591/ijece.v8i5.pp3604-3608.
- [17] Z. M. Ramadan, "Effect of kernel size on Wiener and Gaussian image filtering," *Telkomnika (Telecommunication Computing Electronics and Control)*, vol. 17, no. 3, pp. 1455–1460, Jun. 2019, doi: 10.12928/TELKOMNIKA.v17i3.11192.
- [18] J. Na'am, J. Harlan, R. Syelly, and A. Ramadhanu, "Filter technique of medical image on multiple morphological gradient (MMG) method," *Telkomnika (Telecommunication Computing Electronics and Control)*, vol. 17, no. 3, pp. 1317–1323, Jun. 2019, doi: 10.12928/TELKOMNIKA.v17i3.9722.
- [19] B. Charmouti *et al.*, "An overview of the fundamental approaches that yield several image denoising techniques," *Telkomnika (Telecommunication Computing Electronics and Control)*, vol. 17, no. 6, pp. 2959–2967, Dec. 2019, doi: 10.12928/TELKOMNIKA.v17i6.11301.
- [20] L. Abderrahim, M. Salama, and D. Abdelbaki, "Novel design of a fractional wavelet and its application to image denoising," *Bulletin of Electrical Engineering and Informatics*, vol. 9, no. 1, pp. 129–140, Feb. 2020, doi: 10.11591/eei.v9i1.1548.
- [21] Y. Y. Al-Aboosi, R. S. Issa, and A. K. Jassim, "Image denoising in underwater acoustic noise using discrete wavelet transform with different noise level estimation," *Telkomnika (Telecommunication Computing Electronics and Control)*, vol. 18, no. 3, pp. 1439–1446, Jun. 2020, doi: 10.12928/TELKOMNIKA.V18I3.14381.
- [22] S. Rajkumar and G. Malathi, "An efficient image denoising approach for the recovery of impulse noise," *Bulletin of Electrical Engineering and Informatics*, vol. 6, no. 3, pp. 281–286, Sep. 2017, doi: 10.11591/eei.v6i3.680.
- [23] V. Kishorebabu, P. Ganesan, H. Kamatham, and V. Shankar, "An adaptive decision based interpolation scheme for the removal of high density salt and pepper noise in images," *Eurasip Journal on Image and Video Processing*, vol. 2017, no. 1, p. 67, Dec. 2017, doi: 10.1186/s13640-017-0215-0.

- [24] V. Patanavijit, "Denoising performance analysis of adaptive decision based inverse distance weighted interpolation (DBIDWI) algorithm for salt and pepper noise," *Indonesian Journal of Electrical Engineering and Computer Science*, vol. 15, no. 2, pp. 804–813, Aug. 2019, doi: 10.11591/ijeecs.v15.i2.pp804-813.
- [25] V. Patanavijit and K. Thakulsukanant, "The statistical analysis of random-valued impulse noise detection techniques based on the local image characteristic: ROAD, ROLD and RORD," *Indonesian Journal of Electrical Engineering and Computer Science*, vol. 15, no. 2, pp. 794–803, Aug. 2019, doi: 10.11591/ijeecs.v15.i2.pp794-803.
- [26] N. Singh and U. Oorkavalan, "Triple threshold statistical detection filter for removing high density random-valued impulse noise in images," *Eurasip Journal on Image and Video Processing*, vol. 2018, no. 1, p. 22, Dec. 2018, doi: 10.1186/s13640-018-0263-0.
- [27] A. A. Hussein, S. A. Hussain, and A. H. Reja, "Image mixed gaussian and impulse noise elimination based on sparse representation model," *Indonesian Journal of Electrical Engineering and Computer Science*, vol. 23, no. 3, pp. 1440–1450, Sep. 2021, doi: 10.11591/ijeecs.v23.i3.pp1440-1450.
- [28] D. G. Kim, M. Hussain, M. Adnan, M. A. Farooq, Z. H. Shamsi, and A. Mushtaq, "Mixed noise removal using adaptive median based non-local rank minimization," *IEEE Access*, vol. 9, pp. 6438–6452, 2021, doi: 10.1109/ACCESS.2020.3048181.
- [29] K. N. Hussain, A. K. Naha, and H. K. Khleaf, "A hybrid bat-genetic algorithm for improving the visual quality of medical images," *Indonesian Journal of Electrical Engineering and Computer Science*, vol. 28, no. 1, pp. 220–226, Oct. 2022, doi: 10.11591/ijeecs.v28.i1.pp220-226.
- [30] S. Thomas and A. Krishna, "Impulse noise recuperation from grayscale and medical images using supervised curve fitting linear regression and mean filter," *Indonesian Journal of Electrical Engineering and Computer Science*, vol. 28, no. 2, pp. 777–786, Nov. 2022, doi: 10.11591/ijeecs.v28.i2.pp777-786.
- [31] S. K. Maji and A. Mahajan, "A joint denoising technique for mixed gaussian-impulse noise removal in HSI," *IEEE Geoscience and Remote Sensing Letters*, vol. 20, pp. 1–5, 2023, doi: 10.1109/LGRS.2023.3264522.
- [32] B. A. Hassan and A. A. A. Abdullah, "Improvement of conjugate gradient methods for removing impulse noise images," *Indonesian Journal of Electrical Engineering and Computer Science*, vol. 29, no. 1, pp. 245–251, Jan. 2023, doi: 10.11591/ijeecs.v29.i1.pp245-251.
- [33] V. Jayaraj and D. Ebenezer, "A new switching-based median filtering scheme and algorithm for removal of high-density salt and pepper noise in images," *Eurasip Journal on Advances in Signal Processing*, vol. 2010, no. 1, p. 690218, Dec. 2010, doi: 10.1155/2010/690218.
- [34] V. Patanavijit, D. Kesrarat, W. Lee, K. Srisomboon, and K. Thakulsukanant, "The efficaciousness of the outlier reclamation scheme established on a first-order recursive FIR linear predictor for salt&pepper outlier," in *Proceeding - 12th International Electrical Engineering Congress: Smart Factory and Intelligent Technology for Tomorrow, iEECON 2024*, IEEE, Mar. 2024, pp. 1–4. doi: 10.1109/iEECON60677.2024.10537853.

## BIOGRAPHIES OF AUTHORS



**Voropoj Patanavijit**    received the B.Eng., M.Eng. and Ph.D. degrees from the department of electrical engineering at the Chulalongkorn University, Bangkok, Thailand, in 1994, 1997 and 2007 respectively. He has served as a full-time lecturer at department of electrical and electronic engineering, faculty of engineering, Assumption University since 1998 where he is currently an associate professor. He has authored and co-authored over 180 national/international peer-reviewed publications in digital signal processing (DSP) and digital image processing (DIP). He received the best paper awards from many conferences such as ISCIT2006 (2006), NCIT2008 (2008), EECON-33 (2010), EECON-34 (2011), EECON-35 (2012), and EECON-43 (2020). Moreover, he is invited to be the guest speaker at IWAIT2014 and contributed the invited paper at iEECON 2014. As a technical reviewer of international journals since 2006, he has been assigned to review over 100 journal papers (indexed by SCI and Scopus). As a technical reviewer of over 40 international/national conferences since 2006, he has been assigned to review over 175 proceeding papers. He has participated in more than 8 projects and research programmed funded by public and private organizations. He works in the field of signal processing and multidimensional signal processing, specializing, in particular, on image/video reconstruction, super-resolution reconstruction (SRR), compressive sensing, enhancement, fusion, digital filtering, denoising, inverse problems, motion estimation, optical flow estimation and registration. He can be contacted at email: patanavijit@yahoo.com.



**Kornkamol Thakulsukanant**    received the B.Eng. (electrical engineering) from Assumption University, Thailand in 1994, MSc. (telecommunications and computer network engineering) from London South Bank University, United Kingdom in 1997 and Ph.D. (in electronic and electrical engineering) from Bristol University, United Kingdom in 2009 respectively. She works in the field of digital signal processing (DSP) and digital image processing (DIP), specializing, in particular, on digital image reconstruction/enhancement. She can be contacted at email: kthakulsukanant@yahoo.com.